Am J Physiol Endocrinol Metab 306: E14–E27, 2014.
First published October 29, 2013; doi:10.1152/ajpendo.00155.2013.

Effect of peripherally administered leptin antagonist on whole body metabolism and bone microarchitecture and biomechanical properties in the mouse

Gili Solomon,[1] Ayelet Atkins,[2] Ron Shahar,[2] Arieh Gertler,[1]* and Efrat Monsonego-Ornan[1]*

[1]*Institute of Biochemistry and Nutrition and* [2]*Koret School of Veterinary Medicine, The Robert H. Smith Faculty of Agriculture, Food, and Environment, The Hebrew University, Rehovot, Israel*

Submitted 19 March 2013; accepted in final form 16 October 2013

Solomon G, Atkins A, Shahar R, Gertler A, Monsonego-Ornan E. Effect of peripherally administered leptin antagonist on whole body metabolism and bone microarchitecture and biomechanical properties in the mouse. *Am J Physiol Endocrinol Metab* 306: E14–E27, 2014. First published October 29, 2013; doi:10.1152/ajpendo.00155.2013.—Leptin's in vivo effect on the rodent skeleton depends on the model used and the mode of administration. Superactive mouse leptin antagonist (SMLA) was produced and then pegylated (PEG) to prolong and enhance its in vivo activity. We blocked leptin signaling by injecting this antagonist peripherally into normal mice at various time points and studied their metabolic and skeletal phenotypes. Subcutaneous PEG-SMLA injections into 4-wk-old female C57BL/6J mice increased weight gain and food consumption significantly after only 1 mo, and the effect lasted for the 3 mo of the experiment, proving its central inhibiting activity. Mice showed a significant increase in serum glucose, cholesterol, triglycerides, insulin, and HOMA-IR throughout the experiment. Quantification of gene expression in "metabolic" tissues also indicated the development of insulin resistance. Bone analyses revealed a significant increase in trabecular and cortical parameters measured in both the lumbar vertebrae and tibiae in PEG-SMLA-treated mice in the 1st and 3rd months as well as a significant increase in tibia biomechanical parameters. Interestingly, 30 days of treatment with the antagonist in older mice (aged 3 and 6 mo) affected body weight and eating behavior, just as they had in the 1-mo-old mice, but had no effect on bone parameters, suggesting that leptin's effect on bones, either directly or through its obesogenic effect, is dependent upon stage of skeletal development. This potent and reversible antagonist enabled us to study leptin's in vivo role in whole body and bone metabolism and holds potential for future therapeutic use in diseases involving leptin signaling.

leptin signaling; insulin resistance; microcomputed tomography; obesity

LEPTIN, A 16-KDA PROTEIN, is a central regulator of body weight (BW) (32) as well as a pleiotropic hormone acting both centrally and peripherally. It participates in a variety of biological processes, including energy metabolism, reproduction, and immune response modulation. Obesity is associated with increased leptin synthesis and secretion, whereas fasting and weight loss are associated with decreased leptin synthesis and secretion. Leptin acts through both central and peripheral mechanisms to affect feeding behavior, lipid and glucose metabolism, thermogenesis, reproductive and endocrine functions, and cardiovascular and immune functions (32). The extent of leptin's actions can be seen in *ob/ob* mice that lack leptin in circulation. These mice are obese, diabetic, and sterile and exhibit reduced activity, metabolism, and body temperature. All of these phenotypes can be rescued by daily injection of leptin.

In addition, leptin is a major regulator of bone metabolism, but data are contradictory regarding its effects on bone mass in rodents. Several studies have described leptin-deficient *ob/ob* mice as having high bone mass (4, 24, 46), and intracerebroventricular injections of leptin decrease bone mass in both *ob/ob* mice and lean rodents (25). Others have observed lower bone mass in leptin-deficient mice than in normal mice (35, 85), and studies in *ob/ob* mice have confirmed a stimulatory effect of intraperitoneal leptin administration on bone tissue, specifically a dramatic increase in cortical bone formation (85). From these conflicting findings, it is tempting to hypothesize that leptin exerts multiple effects, depending on bone tissue, skeletal maturity, and/or signaling pathway. Thus, during the postnatal stage of development, leptin might stimulate bone growth and bone size through direct angiogenic and chondro-osteogenic effects (51, 60). However, at a later stage, it may decrease bone remodeling in the mature skeleton, when trabecular bone turnover is high, by stimulating the osteoprotegerin/RANK/ligand pathway (88). Leptin also exerts negative effects on bone formation through a hypothalamic pathway. The hypothalamic leptin-dependent antiosteogenic and anorexigenic networks differ, and the peripheral mediators of leptin antiosteogenic function are neuronal. Leptin deficiency results in low sympathetic tone, and genetic or pharmacological ablation of adrenergic signaling leads to a leptin-resistant high bone mass, with no effect on the anorexigenic axis (87). The two pathways might counterbalance each other, with the peripheral and positive effects being predominant when central leptin resistance occurs with the onset of obesity. Ducy et al. (24) showed thicker trabeculae in 3- and 6-mo-old *ob/ob* and *db/db* mice compared with wild-type (WT) mice and increased bone formation rate by affecting cortical bone. Similarly, histomorphometric quantitation showed a nearly twofold increase in trabecular bone volume in *ob/ob* and *db/db* mice compared with their WT littermates. Furthermore, biomechanical analysis of long bones of 6-mo-old *ob/ob* mice, WT mice, and ovariectomized (WT-OVX) mice revealed that *ob/ob* mice have stiffer bones than WT-OVX animals, indicating that leptin is a major regulator of bone formation through central regulation of bone remodeling (24). Ducy et al. (24) concluded that this high bone mass phenotype, affecting all bones in the body, is due to a massive increase in bone formation. In contrast, Hamrick and colleagues (35, 36) and Steppan et al. (85) argued that although *ob/ob* mice show increased spinal trabecular density [bone volume/tissue volume (BV/TV)], they have significantly lower whole body bone mineral content and bone mineral density (BMD) compared with normal mice. *ob/ob* and *db/db* mice showed lower femoral bone mass and

* Both of these authors contributed equally to this article.
Address for reprint requests and other correspondence: E. Monsonego-Ornan, Inst. of Biochemistry and Nutrition, The Robert H. Smith Faculty of Agriculture, Food, and Environment, The Hebrew University, P. O. Box 12, Rehovot 76100, Israel (e-mail: efrat.mo@mail.huji.ac.il).

BMD than normal mice because of a reduction in cortical thickness and trabecular density (BV/TV) (35, 36, 85). In this case, leptin injection is expected to increase femur length and BMD in these animals.

The function of leptin is not restricted to rodents. Pogoda et al. (68) showed that leptin controls bone formation by reducing trabecular bone in sheep. Elefteriou et al. (25) showed that lipodystrophic patients who displayed low to undetectable circulating levels of leptin had marked advances in bone age. The same advance in bone age was also observed in a single leptin-deficient child. These correlative data suggest that serum leptin in humans also controls bone homeostasis (25) through its effects on the process of bone development in the postnatal period.

Random mutagenesis of leptin, followed by selection of high-affinity mutants coupled with alanine mutagenesis of three amino acids (L39A/D40A/F41A) (80), produced a potent antagonist of leptin activity (D23L/L39A/D40A/F41A) that competes with the WT hormone for binding to leptin receptors. This antagonist was termed superactive mouse leptin antagonist (SMLA) (82). Compared with unmodified leptin, SMLA exhibited a >60-fold increased binding to leptin receptor and 14-fold higher antagonistic activity in vitro relative to the L39A/D40A/F41A mutants. To prolong and enhance its in vivo activity, SMLA was monopegylated at the NH_2 terminus and termed pegylated (PEG)-SMLA. We demonstrated previously that this protein, injected subcutaneously (sc) into either male or female mice, induces very potent and rapid weight gain activity, leading to a 45–50% increase in body mass in 2 wk (82). Moreover, upon cessation of leptin antagonist injection, the weight decreased to that of the control mice within 10–14 days (27). We hypothesize that blocking leptin action by PEG-SMLA may lead to the creation of a novel, rapid model of metabolic syndrome and maybe even of type 2 diabetes mellitus (T2DM). Blocking leptin action in WT mice at different ages may also lead to a better understanding of leptin's involvement in bone metabolism.

MATERIALS AND METHODS

Animals. The studies were approved by The Hebrew University of Jerusalem Animal Care and Use Committee, Ethics No. MD-10-12675-2. Female C57BL/6J WT mice (10 g, 3 wk old) were purchased from Harlan Laboratories (Jerusalem, Israel). The mice were acclimatized for 1 wk and fed a normal chow diet. They were housed four per cage in a temperature- (21–22°C) and light-controlled (lights on from 0800 to 1800) room. Food (Harlan Laboratories) and water were provided ad libitum to all animals. For the two short-term experiments, 2- and 3-mo-old female C57BL/6J WT mice weighing 17.5 and 18.5 g initial weight, respectively, at *time zero* were purchased from Harlan Laboratories.

Experimental design. Animals were 4 wk old at the beginning of the experiment, which lasted 3 mo. At the end of the 1st and 3rd months, a group of control mice and a group of treatment mice (n = 11 from each group) were euthanized. The control group was injected sc with saline. The treated group was injected sc with 10 mg PEG-SMLA/kg BW, but only every other day, because pegylation increases the half-life of the leptin antagonist, resulting in significantly increased bioavailability and retention of antagonistic activity (27). Mouse and food weights were monitored every 4 days to calculate weight gain and food consumption.

On *days 20* and *26* of the 1st and 3rd months, the mice were injected sc with calcein (15 mg/kg) and alizarin complexone (10 mg/kg; both from Sigma Chemical, St. Louis, MO) consecutively to label mineralizing bone for assessment of bone formation rates.

Tissue collection and analyses. The animals were anesthetized with isoflurane and euthanized by cervical dislocation. Vertebrae, femurs, and tibias were excised, wrapped in saline-wetted gauze, and frozen at −20°C until subsequent microcomputed tomography (μCT) and histomorphometry analyses. Abdominal white adipose tissue (WAT), liver, muscle, and brain were removed and frozen in liquid nitrogen before being stored at −80°C for gene expression analysis.

Serum assay. Blood was collected via the abdominal aorta in anesthetized animals prior to euthanization, allowed to clot in tubes chilled on ice for 30 min, and centrifuged, and the serum was removed and stored frozen at −80°C for hormone analyses. Serum insulin was assayed in duplicate using the Mercodia Ultrasensitive mouse insulin ELISA (Uppsala, Sweden) according to the manufacturer's instructions. The assay sensitivity was 0.0025 μg/l. Other blood parameters were analyzed by American Medical Laboratories (Herzliya, Israel).

Real-time PCR gene quantification. Total RNA was isolated from WAT, liver, muscle, and brain using Tri Reagent (Molecular Research, Cincinnati, OH) according to the manufacturer's protocol. Total RNA (1 μg) was reverse transcribed using a High Capacity cDNA kit (Applied Biosystems, Foster City, CA). cDNA was diluted 1:25 and used for real-time PCR with a Platinum SYBR Green quantitative PCR SuperMix-UDG with ROX (Applied Biosystems) and specific primer sets (Table 2) to measure gene expression. Dissociation curves were constructed following real-time PCR to ensure detection of the desired amplicon and exclude the presence of contaminating products. Amplification was carried out using a 7300 Fast Real-Time PCR System (Applied Biosystems). Gene expression was normalized to that of GAPDH, and the data were analyzed using the comparative $2^{-\Delta\Delta C_T}$ method (47).

μCT analyses. Third and fourth lumbar vertebrae (LV3 and LV4, respectively) and tibiae were scanned with a Skyscan 1174 X-ray μCT scanner (Skyscan, Aartselaar, Belgium) equipped with a charge-coupled device detector. Images were obtained by 50 kVp X-ray tube potential and 800 mA X-ray tube current. Scans were obtained using a 0.25-mm aluminum filter, 4,300-ms integration time, at 11.1 μm^3 isotropic voxel size. For each specimen, a series of 900 projections were obtained with a rotation step of 0.4°, using two-frame averaging for a total 360° rotation. Flat-field correction was performed at the beginning of each scan for a specific zoom and image format. A stack of two-dimensional X-ray shadow projections was reconstructed using Nrecon Skyscan software, version 1.6.1.2, and subjected to morphometric analysis by CT analyzer Skyscan software, version 1.9.3.2. During reconstruction, dynamic image range, post-alignment value, beam hardening, and ring artifact reduction were optimized. Analysis of the middiaphyseal cortex of the tibia was carried out from the chondro-osseous junction toward the midshaft by subtracting 20 slices corresponding to 0.222 mm and then measuring a region of interest (ROI) consisting of 150 slices, corresponding to a 1.665-mm cortical segment. Cortical analysis of the LV3 was evaluated in the region where the right transverse process connects to the vertebrae body; deducting 50 slices corresponds to 0.555 mm and measuring a ROI consisting of 30 slices corresponds to a 0.033-mm cortical segment. Vertebral cortical analysis was computed by manually delineating the ventral vertebral cortex for 30 slices of the cranial vertebral body. Trabecular analysis was carried out on the bodies of LV3 and LV4. Trabecular bone was evaluated in the region where the right transverse process connects to the vertebra body by subtracting 30 slices corresponding to 0.333 mm and measuring a ROI consisting of 150 slices corresponding to a 1.665-mm trabecular segment. Trabecular analysis of the proximal tibia metaphysis began 20 slices distal to the densest slice of the physis, as determined by visual inspection. The next 30 distal slices corresponding to 0.333 mm were contoured and subsequently analyzed. Trabecular bone morphological parameters included trabecular BV/TV (%), trabecular number (1/μm), trabecular thickness (μm), and trabecular separation (μm). For visual demon-

stration, three-dimensional images (CTM file format) were constructed from cortical and trabecular ROIs, utilizing Marching Cubes 33 algorithm in CTVol software.

Biomechanical testing. Following μCT scanning, tibiae were subjected to biomechanical testing using a custom-built, saline-containing, micromechanical device. All bones were tested by three-point bending method while fully immersed in saline. Each bone was placed such that the diaphysis of the caudal orientation was between the two stationary supporting anvils of the mechanical testing device. The distance between the stationary supports was 8 mm to ensure that the relatively tubular portion of the middiaphysis rests on these supports. An initial preload of 0.2 N was applied to hold the bone in place. Loading proceeded at a constant rate of 500 μm/min to the fracture point, as identified by a sudden decrease in load. Force displacement data were collected by a custom Labview routine. The resulting load-displacement curves were used to calculate whole bone stiffness (slope of the linear portion of the load-displacement curve), maximal load, yield load, and area under the curve (AUC). The yield point was defined as the load at which the load-deformation relationship ceases to be linear and was determined by adapting the 0.03% offset criterion (89).

Sample preparation and dynamic histomorphometry. Femurs were fixed overnight in 4% paraformaldehyde (Sigma-Aldrich, St. Louis, MO) in PBS at 4°C following dehydration in graded ethanol solutions and embedded in glycol methacrylate (JB-4 Embedding Kit; EMS, Hatfield, PA) according to the manufacturer's protocol. The middiaphysis was cut into 5-μm transverse slices using a Leica RM 2255 (Nussloch, Germany) microtome and mounted on Superfrost slides (Thermo Scientific, West Palm Beach, FL). Fluorochromes were observed using confocal laser scanning microscopy (Leica DMI4000B; Leica, Wetzlar, Germany) equipped with Leica Application Suite software. Micrographs were taken using ×10 and ×43 objectives. The excitation wavelength for calcein was set to 488 nm, whereas the emission was measured from 505 to 530 nm. The excitation wavelength for alizarin complexone was set to 532 nm, with emission measured in a range of 660 to 760 nm.

Liver tissue staining. Liver tissues were embedded in optimum cutting temperature (OCT) compound (Sakura, Tokyo, Japan), frozen at −80°C, sectioned to 8 μm with a cryostat (Leica CM1850), and mounted on Superfrost slides. The samples were stained with Oil Red O (Sigma-Aldrich) and examined under a Nikon Eclipse E400 microscope equipped with an Olympus D71 camera and cell A software.

Statistical analysis. All data are expressed as means ± SE. The significance of differences between groups was determined using JMP 7.0 Statistical Discovery Software (SAS Institute 2000) by one-way analysis of variance. Differences between groups were further evaluated by Tukey-Kramer honestly significantly different test. Differences were considered significant at $P < 0.05$.

RESULTS

Short-term experiments using mouse leptin antagonist and PEG-mouse leptin antagonist. Binary relatively short-term (30-day) experiments were conducted using female C57BL/6J WT mice. MLA was administered in two daily injections (800 μg/day) commencing at the age of 8 wk in the first experiment and at the age of 12 wk in the second experiment. PEG-mouse leptin antagonist (MLA) was similarly administered at 250 μg/day once/day. As an additional control, a group of mice were injected with mouse leptin or PEG mouse leptin (at 2 × 10 and 20 μg/day, respectively). As shown in Fig. 1*A*, mice given MLA gained ~10% more weight than controls compared with ~25% more weight gain in mice injected with PEG-MLA (Fig. 1*C*). In both experiments, major weight gain and a parallel increase in abdominal fat (not shown) were achieved in the first 6–10 days of the experiments and were attributed to increased food intake (Fig. 1, *B* and *D*). Leptin treatment in *experiment 1* resulted in a small weight decrease that lasted only for the first 6 days (Fig. 1*A*), whereas administration of PEG leptin in *experiment 2* (Fig. 1*C*) resulted in ~15% weight loss within 7 days that lasted until the end of the experiment. Leptin antagonist-treated mice had significantly higher serum cholesterol levels than leptin-treated mice, but levels were not statistically different from those of the control group. Serum triglyceride levels did not differ among the three groups. Serum glucose was significantly lower in the leptin-treated mice compared with the control group but was not different in leptin antagonist-treated mice compared with controls. In both experiments, we tested the effect of leptin antagonist treatment

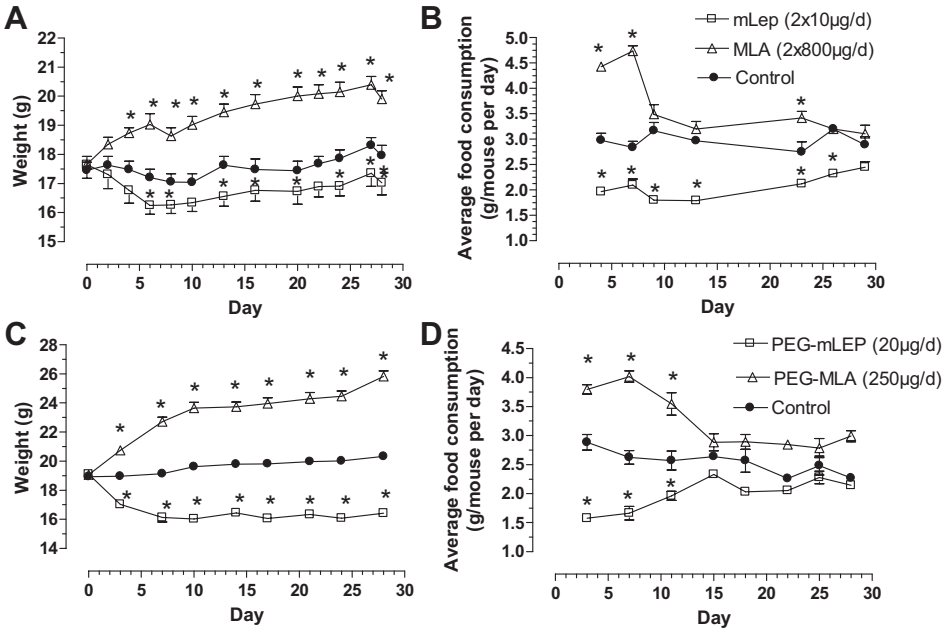

Fig. 1. Weight gain (*A*) and food consumption (*B*) in mice injected sc with mouse leptin (mLep; 2 × 10 μg/day), mouse leptin antagonist (MLA; 2 × 800 μg/day), and saline as a control (200 μl) for 30 consecutive days. Weight gain (*C*) and food consumption (*D*) of mice injected sc with pegylated (PEG)-mLep (20 μg/day), PEG-MLA (250 μg/day), and saline as control (200 μl) for 30 consecutive days. Data show means ± SE. *$P < 0.05$ (compared with control); $n = 12$.

on bone parameters and found it to be insignificant or minor compared with results shown in *ob/ob* mice (24).

Long-term PEG-SMLA treatment dramatically increased BW and food consumption in WT mice. To further test the effects of leptin antagonists on both metabolic and bone parameters, an additional experiment lasting 12 wk was performed. In this experiment, we used younger (4-wk-old) female WT mice to elucidate the effect of early leptin signaling on bone and metabolic parameters. Instead of PEG-MLA or MLA, we employed the recently developed PEG-SMLA, which shows 7- to 27-fold more potent (compared with PEG-MLA) activity in vivo (82). Four-week-old female C57Bl/6J mice were randomly divided into four groups, each consisting of 10 or 11 animals. Two groups were injected sc every other day with PEG-SMLA (10 mg/kg) and two others with saline; the experiment was terminated after 4 and 12 wk, respectively.

Analysis of weight gain and food consumption during the 12-wk experiment showed a dramatic weight increase in PEG-SMLA-treated mice from *day 3* to approximately *day 20*, after which the weight gain slowed down (Fig. 2*A*). These data suggest compensatory development of a state of enhanced leptin sensitivity in contrast to the relative leptin resistance noted in hyperleptinemic morbid obesity (62). Weight gain in PEG-SMLA-treated mice was associated with a significant increase in food consumption that was elevated at the beginning of the treatment and decreased with time to slightly above control levels, although weight continued to increase (Fig. 2*B*). The average amount of food eaten by the mice in the first month and over the whole experiment was calculated, demonstrating the hyperphagic phenotype of the antagonist-injected mice that consumed 118 $g \cdot mouse^{-1} \cdot mo^{-1}$ (366 $kcal \cdot mouse^{-1} \cdot mo^{-1}$) in the 1st month of the experiment and 291 g/mouse (901 kcal/mouse) during the whole experiment. While in the control group, food consumption was 72 $g \cdot mouse^{-1} \cdot mo^{-1}$ (224 $kcal \cdot mouse^{-1} \cdot mo^{-1}$) in the 1st month of the experiment and 203 g/mouse (631 kcal/mouse) during the whole experiment. The average caloric intake per BW during the experiment was calculated to estimate the efficiency of energy utilization, revealing differences between the groups. Energy consumption per BW was lower in the antagonist-injected mice (28 kcal/g of BW) compared with control (34 kcal/g of BW), suggesting that blocking leptin increased food consumption and reduced energy expenditure.

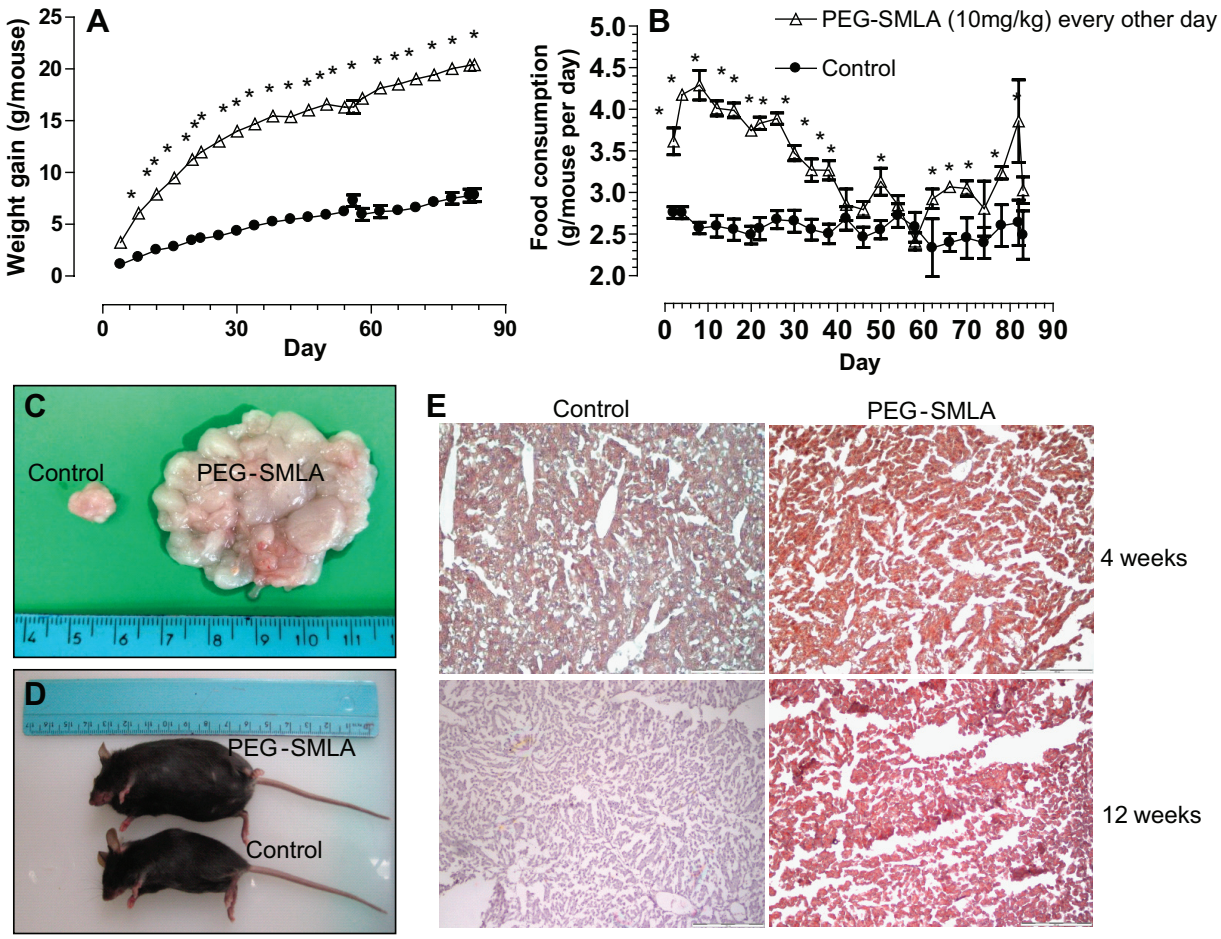

Fig. 2. Inhibition of leptin signaling by PEG-superactive mouse leptin antagonist (SMLA). *A*: weight gain (means ± SE; $n = 11$) in 4-wk-old female C57BL/6J mice during 12 wk of sc PEG-SMLA (10 mg/kg) or saline (control) injection every other day. Initial weight at *time zero* was 12 g. *B*: average daily food consumption of female C57BL/6J mice injected sc with PEG-SMLA (10 mg/kg) or saline (control) calculated for every 3 days. Treatment vs. control; $*P < 0.05$. *C*: visceral fat from representative PEG-SMLA-treated and control mice at the end of the 12-wk experiment. *D*: appearance of representative control and PEG-SMLA-treated 16-wk wk-old mice. *E*: histological analyses of frozen 8-μm cryosections of liver tissue embedded in optimum cutting temperature compound stained with Oil Red O at the end of 4 and 12 wk of treatment; magnification ×10.

Obesity and visceral fat accumulation were demonstrated at the end of the 4- (not shown) and 12-wk experiments in 16-wk-old mice (Fig. 2, *C* and *D*). These data show that leptin was indeed inhibited by PEG-SMLA through central regulation. Histological analyses of 8-μm cryosections of liver tissue embedded in OCT compound and stained with Oil Red O at the end of 4 and 12 wk of treatment indicated fatty liver in PEG-SMLA-treated mice (Fig. 2*E*).

To characterize the metabolic status of PEG-SMLA-treated mice throughout the 12 wk of experimentation, a complete blood profile was performed after 4 and 12 wk of treatment (Table 1). Weight gain was accompanied by elevated glucose, cholesterol, and triglyceride levels, and an even more dramatic increase in insulin levels and insulin resistance as calculated by homeostasis model assessment-insulin resistance (HOMA-IR). PEG-SMLA did not affect other blood parameters such as albumin, globulin, creatinine, urea, calcium, potassium, phosphorus, or bilirubin (data not shown).

Insulin and glucose levels can indicate whether mice in the experimental treatment are normal, are insulin resistant, or have developed T2DM according to the following criteria: in normal mice, glucose and insulin levels are <1.95 SD above control average; in insulin-resistant mice, insulin level is >1.95 SD above control average, but glucose is <1.95 SD above control average; in mice with T2DM, both insulin and glucose are >1.95 SD above control average. With respect to insulin levels, the results show that all six values of mice given PEG-SMLA were above the 1.39 ng/ml insulin limit at the end of 4 wk of treatment (Fig. 3*A*), and nine out of 10 values of mice given PEG-SMLA were above the 0.60 mg/ml insulin limit at the end of the 12-wk treatment (Fig. 3*B*). A determination of glucose levels showed that after 4 wk of treatment, four out of eight values of mice given PEG-SMLA were above the 212 mg/100 ml limit (Fig. 3*C*), and three out of 10 values of mice given PEG-SMLA were above the 179 mg/100 ml limit at the end of the experiment (Fig. 3*D*). These data suggest that the PEG-SMLA-treated mice have already developed insulin resistance after 4 wk of PEG-SMLA treatment but are only marginally diabetic. Furthermore, prolonged treatment with PEG-SMLA did not lead to increased numbers of diabetic mice.

The effect of PEG-SMLA treatment on gene expression in adipose tissue, brain, liver, and muscle. To gain a better understanding of the effect of blocking leptin on the metabolic state of the mice, we evaluated gene expression patterns in tissues from mice treated with PEG-SMLA for 4 and 12 wk. RNA was isolated from fat (WAT), liver, muscle, and brain, followed by quantitative real-time PCR. The results are summarized in Supplemental Table S1 (Supplemental Material for this article can be found online at the *AJP-Endocrinology and Metabolism* website).

The effect on gene expression in WAT. The most dramatic effect was found in the expression of the leptin gene, which was increased dramatically after 4 wk and even more after 12 wk of treatment, whereas the expression of the leptin receptor gene decreased significantly after 4 wk but did not change further up to 12 wk, implying local regulation of leptin and its receptor's expression by blocking leptin. Adiponectin gene expression was surprisingly increased after 12 wk. PEG-SMLA treatment also partially affected the adipogenesis/lipogenesis pathways. *PPARγ* expression was upregulated five- and twofold after 4 and 12 wk of treatment, consistent with the fact that it causes suppression of insulin action and promotes insulin resistance. However, it happened without the expression of insulin receptor being changed.

Expression of lipoprotein lipase (*LPL*), which is known to be upregulated by insulin and may predispose toward fat gain, was also increased after 4 and 12 wk. Expression of other lipogenesis-related enzymes such stearoyl-CoA desaturase 1 (*SCD1*) and *RIFL* (the novel refeeding fat and liver protein) was significantly elevated after 12 wk of treatment. Surprisingly, expression of fatty acid synthase (*FASN*) was reduced significantly after 12 wk, whereas expression of several other tested genes was not changed. PEG-SMLA treatment reduced the expression of several genes related to glucose metabolism such as glucose transporter 4 (*GLUT4*) and phosphofructokinase after 4 wk of treatment, in which the fast weight gain was observed, whereas pyruvate dehydrogenase kinase 1 (*PDK1*), which inactivates the pyruvate dehydrogenase complex, decreased significantly only after 12 wk.

Mitochondrial thermogenesis was affected partially by PEG-SMLA treatment, as shown by upregulation of uncoupling proteins 2 and 3 (*UCP2* and *UCP3*, respectively) after 4 wk of treatment, whereas the upregulation after 12 wk was lesser and not statistically significant. There was also some nonsignificant decrease in expression of apoptosis-related proteins. Twelve weeks of PEG-SMLA treatment also resulted in elevated expression of TNFα but not other inflammation-related proteins, indicating a mild inflammatory state. As expected, expression of sirtuin 1 (*SIRT1*), which is known to be downregulated in cells having high insulin resistance, was reduced three- and twofold after 4 and 12 wk of treatment, respectively. Recently, the prohibitin (*PHB*) gene has been found to modulate mitochondrial fuel metabolism in adipocytes by specifically inhibiting the activity of pyruvate carboxylase; moreover, leptin-treated *ob/ob* mice showed downregulated expression of pyruvate carboxylase (90). *PHB* expression was upregulated 2.5-fold

Table 1. *Biochemical and hormonal parameters in 8-wk-old female mice (after 4 wk of treatment) and in 16-wk-old female mice (after 12 wk of treatment) injected sc with PEG-SMLA at 10 mg·kg^{-1}·day^{-1} (injected every other day)*

	4 wk		12 wk	
	Control	PEG-SMLA	Control	PEG-SMLA
Glucose, mg/dl	188.6 ± 15.0	237 ± 21.4	131.1 ± 7.7	183.3 ± 10.4*
Cholesterol, mg/dl	95.8 ± 8.1	147.6 ± 14.9**	105.4 ± 5.5	153 ± 3.7**
Triglycerides, mg/dl	97 ± 11.9	153.5 ± 15.34*	92.5 ± 6.06	121.7 ± 9.54*
Insulin, ng/ml	0.8 ± 0.13	4.11 ± 0.7***	0.31 ± 0.05	1.84 ± 0.3***
HOMA-IR	57.2 ± 9.4	380.1 ± 90***	17.7 ± 4.15	139.5 ± 27.8***

Data show means ± SE; $n = 11$. PEG-SMLA, pegylated-superactive mouse leptin antagonist; HOMA-IR, homeostasis model of assessement-insulin resistance. *$P < 0.05$, **$P < 0.01$, and ***$P < 0.001$ vs. control.

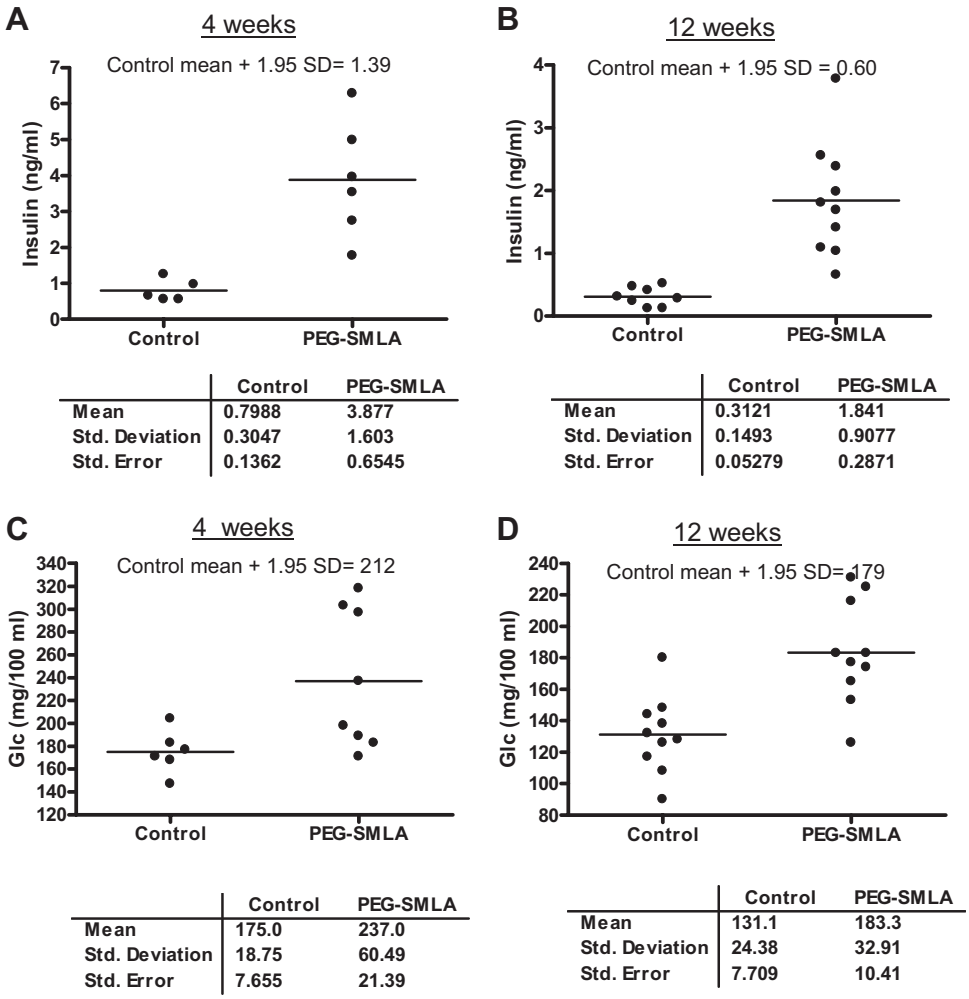

	Control	PEG-SMLA
Mean	0.7988	3.877
Std. Deviation	0.3047	1.603
Std. Error	0.1362	0.6545

	Control	PEG-SMLA
Mean	0.3121	1.841
Std. Deviation	0.1493	0.9077
Std. Error	0.05279	0.2871

	Control	PEG-SMLA
Mean	175.0	237.0
Std. Deviation	18.75	60.49
Std. Error	7.655	21.39

	Control	PEG-SMLA
Mean	131.1	183.3
Std. Deviation	24.38	32.91
Std. Error	7.709	10.41

Fig. 3. Development of insulin resistance and type 2 diabetes mellitus in mice treated for 4 or 12 wk with PEG-SMLA (10 mg/kg every other day), as determined by measuring blood glucose and insulin levels and calculating the no. of animals having values higher than the mean + 1.95 SD of the control mice. *A*: all values of mice injected with 10 mg/kg PEG-SMLA every other day are above the 1.39 ng/ml limit for insulin. *B*: 9 of 10 mice injected with 10 mg/kg PEG-SMLA every other day were above the 0.60 ng/ml limit for insulin. *C*: 4 of 8 mice injected with PEG-SMLA were above the 212 mg/100 ml limit for glucose (Glc). *D*: 3 of 10 mice injected with PEG-SMLA were above the 179 mg/100 ml limit for glucose.

after 4 but not 12 wk. Protein disulfide isomerase-associated 3 (*PDIA3*) is involved in the mitogen-activated protein kinase (*MAPK*) signaling cascade that is activated by leptin (33). *PDIA3* gene expression, which is known to be upregulated by leptin-injected *ob/ob* mice (93), was significantly downregulated.

The effect on gene expression in brain. Because of the technical difficulty involved in accurately isolating the hypothalamus, the whole brain was taken for RNA extraction to study genes related to energy expenditure and food intake. The expression of the *SIRT1* gene did not change significantly after 4 wk but was reduced threefold after 12 wk. Reduced hypothalamic *SIRT1* expression has been shown to suppress food intake in rodents due to diminished *SIRT1* activity in agouti-related peptide (*AgRP*) neurons (10, 22). Blocking leptin by PEG-SMLA treatment resulted in slightly reduced expression of the genes encoding the anorexigenic peptides (81) apolipoprotein E (*apoE*) and proopiomelanocortin (*POMC*) after 12 but not 4 wk. In parallel, gene expression of neuropeptide Y (*NPY*) and *AgRP*, which are known to increase energy expenditure and food intake, respectively (57), showed significant upregulation for the former only after 4 wk, whereas *AgRP* expression did not change at all. Reduction of thermogenesis-related protein *UCP2* and *UCP3* was observed after 4 wk only.

The effect on gene expression in liver. Gene expression in the liver was tested to determine how leptin inhibition influences lipogenesis, gluconeogenesis, and glycolysis. *SCD1* expression increased significantly, by 3.1- and 4.6-fold after 4 and 12 wk, and that of *Agpat2* increased twofold after 4 wk only. *LPL* gene expression decreased more than threefold after 4 wk but returned to control levels after 12 wk, whereas expression of other genes as well as genes related to cholesterol synthesis remained unchanged. Expression of liver X receptor that may influence the development of metabolic disorders was reduced after 4 wk despite the appearance of the metabolic syndrome. In view of insulin resistance, an increase in gluconeogenesis could be expected, but expression of all four gluconeogenesis-related genes did not increase significantly, and expression of phospho*enol*pyruvate carboxykinase (*PEPCK*) and PPARγ coactivator-1α (*PGC-1α*) even decreased after 4 and 12 wk, respectively, of PEG-SMLA treatment. Of the five genes related to glycolysis, only aldolase A and pyruvate dehydrogenase phosphatase catalytic subunit 2 showed significant decreases in expression after only 4 wk. PEG-SMLA treatment downregulated *CD14* gene expression. Toll-like receptor 4 was slightly downregulated, but the decrease was statistically borderline. fibroblast growth factor 21 (*FGF21*) gene expression was not changed after 4 wk but showed a fivefold decrease after 12 wk. No changes were observed in other tested genes.

The effect on gene expression in muscle. Gene expression in the muscle was tested to determine how leptin inhibition

influences insulin and leptin receptor expression, glycolysis and gluconeogenesis pathways, and thermogenesis. Skeletal muscle is the major tissue responsible for glucose uptake and metabolism in the postprandial state, and glucose transport is a rate-limiting step for glucose uptake and metabolism in insulin-sensitive tissue such as skeletal muscle. *GLUT4* gene expression increased significantly after 4 wk and returned to normal levels after 12 wk. *GLUT1*, which is also expressed in skeletal muscle, is generally believed to play a negligible role in glucose transport and does not appear to be involved in insulin-mediated glucose transport in skeletal muscle (23); its gene's expression was reduced after 12 wk. The gene expression of key enzymes affecting glycolysis showed no change for *PFK* and a decrease after 12 wk for *PDK1*. This suggests that the skeletal muscle did not show the insulin resistance phenotype. Expression of *UCP3* increased threefold after 4 wk, and it could be responsible for *GLUT4*-elevated expression after 4 wk. Gene expression of *SIRT1*, which in myocytes has been suggested to upregulate fatty acid oxidation and enhances O_2 consumption as well as expression of *PPARδ*, decreased significantly after 12 wk. Leptin receptor was reduced 1.5-fold after 12 wk, whereas expression of other tested genes did not change significantly.

The effect of long-term PEG-SMLA treatment on bone morphology. We used μCT scanning to evaluate whether the lack of leptin signaling and the subsequent metabolic state influence the geometric parameters of the bones (Fig. 4, *A–F*). Trabecular bone parameters were measured in lumbar vertebral bodies and proximal tibia metaphysis. Cortical bone parameters were measured in the ventral vertebral cortex of the cranial vertebral body and cortical bone parameters in the midshaft of the tibia.

PEG-SMLA treatment increased BV/TV. The structural characteristics of trabecular bone from the two groups are presented in Table 2. Bone volume fraction, mean trabecular thickness, and trabecular number were all higher in the PEG-SMLA-treated mice compared with the control group in the two tested vertebrae, LV3 and LV4, after 4 and 12 wk of treatment. All of these results were statistically significant except for the mean trabecular thickness in LV4, which was slightly (but not significantly) higher in the PEG-SMLA-treated mice compared with the control group at the end of the 1st and 3rd months of treatment. Bone volume fraction (BV/TV) was elevated by 31 and 28% after 4 and 12 wk, respectively, in LV3, and by 26 and 25% after 4 and 12 wk, respectively, in LV4. Trabecular number was higher by 22–23%, whereas trabecular thickness was higher by only 4–7% in the treated mice. Similarly, in the earlier mouse experiment, trabecular number was increased by 12% in the PEG-MLA-treated group compared with the PEG-leptin group. At this stage of life, when the bone is still developing, a 25–30% elevation in BV/TV represents an important role for leptin signaling in bone modeling and development. BV/TV was elevated by 11 and 24% after 4 and 12 wk, respectively, in trabecular area at the proximal tibia. Trabecular thickness and trabecular number were significantly elevated only after 12 wk of treatment.

PEG-SMLA treatment positively affected cortical morphological characteristics. The morphological characteristics of tibial and vertebral cortical bones from the two groups are presented in Table 3. In tibia, area inside the periosteum, cross-sectional area, medullary area, and polar moment of inertia were significantly higher in the PEG-SMLA-treated group than in the control group at the end of the 1st and 3rd months of treatment. However, no significant changes were detected in cortical thickness, and mean BMD was decreased in the PEG-SMLA-treated mice. In vertebrae, cortical thickness and BMD were significantly higher in the PEG-SMLA-

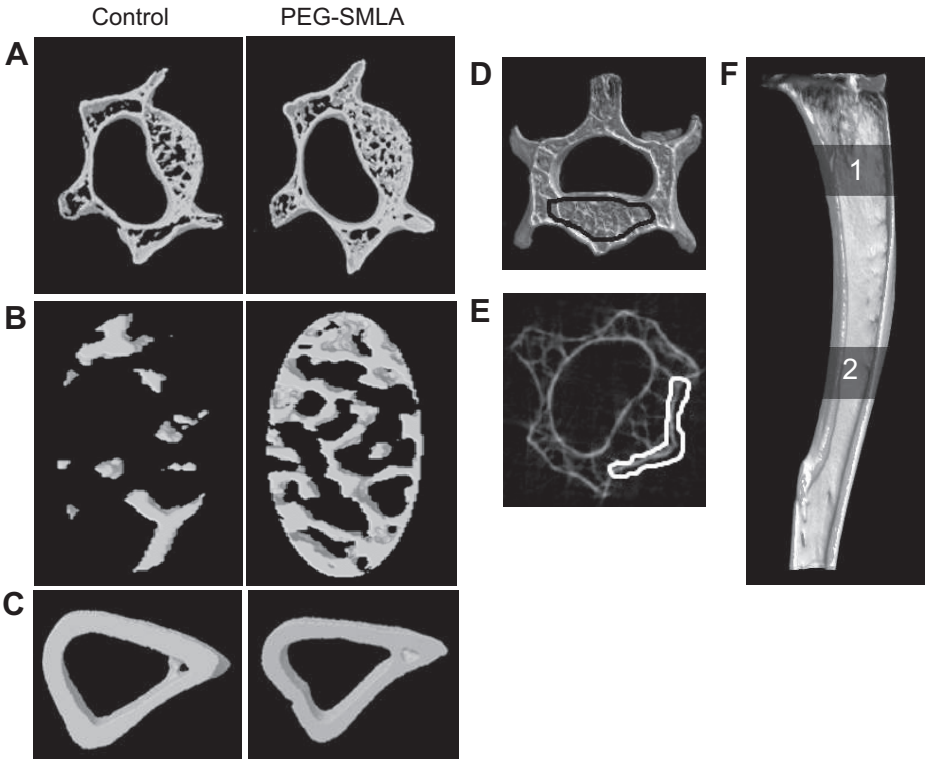

Fig. 4. *A–C*: microcomputed tomography (μCT) 3D images of representative trabecular and cortical bone from PEG-SMLA-treated mice (10 mg/kg every other day) and control at the end of 4 wk of treatment. *A*: 3rd lumbar vertebrae (LV3). *B*: transverse section of LV3; note the increased trabecular bone volume fraction in PEG-SMLA treated group. *C*: image of representative cortical bone from tibia of control and PEG-SMLA-treated groups. *D*: 2D μCT image showing region of trabecular bone evaluation in the LV3. *E*: 2D μCT image showing outlined region of cortical bone in the vertebral body. *F*: 3D μCT image of representative longitudinal section of tibia. Trabecular area analyzed (*1*) and cortical area analyzed (*2*) are represented.

Table 2. *Morphological characteristics of LV3 and LV4 at the end of the 1st and 3rd months of treatment*

	4 wk		12 wk	
	Control	PEG-SMLA	Control	PEG-SMLA
LV3				
BV/TV, %	16.5 ± 1.2	21.61 ± 0.8*	13.74 ± 0.6	17.6 ± 0.4*
Tb.Th, μm	0.068 ± 0.001	0.073 ± 0.0009*	0.068 ± 0.001	0.073 ± 0.0007*
Tb.Sp, μm	0.25 ± 0.01	0.22 ± 0.01*	0.32 ± 0.007	0.28 ± 0.006*
Tb.N, 1/μm	2.41 ± 0.13	2.96 ± 0.1*	1.99 ± 0.08	2.42 ± 0.06*
LV4				
BV/TV, %	15.6 ± 0.9	19.7 ± 0.7*	13.8 ± 0.7	17.2 ± 0.6*
Tb.Th, μm	0.07 ± 0.001	0.073 ± 0.001	0.071 ± 0.001	0.073 ± 0.001
Tb.Sp, μm	0.28 ± 0.01	0.25 ± 0.001*	0.34 ± 0.02	0.31 ± 0.01*
Tb.N, 1/μm	2.2 ± 0.1	2.7 ± 0.09*	1.95 ± 0.1	2.36 ± 0.08*

Data show means ± SE; $n = 11$.LV3, 3rd lumbar vertebrae; LV4, 4th lumbar vertebrae; BV/TV, bone volume/tissue volume; Tb.Th, trabecular thickness; Tb.Sp, trabecular separation; Tb.N, trabecular number. *$P < 0.05$ vs. control.

treated group compared with the control group only at the end of the first month of treatment.

PEG-SMLA treatment positively affected mechanical properties. Based on the modifications observed in bone morphology, we anticipated that PEG-SMLA-treated bones would also show changes in their mechanical properties. To verify this, we tested tibiae by three-point bending (Table 4). Significant differences were found in the mechanical properties of the tibiae between the two groups, mainly at the end of the 1st month ($P < 0.05$). PEG-SMLA-treated bones had significantly higher maximal load, whole bone stiffness, AUC (which is a measure of the energy required to fracture the bone), and yield load compared with the control group. Load to fracture also showed a tendency to be higher, but the difference was not statistically significant.

At the end of the 3-mo experiment, yield load was significantly higher in the PEG-SMLA-treated group, and maximal load and stiffness were also higher and nearly significant ($P < 0.06$), whereas AUC and load to fracture were higher but did not reach statistical significance. These findings suggested that bones from the PEG-SMLA group were stiffer and required more energy to fracture.

Long-term PEG-SMLA treatment positively affected mineral apposition rate. To further elucidate the mode of action of leptin signaling on bone morphology, we monitored the dynamics of bone formation following injection of two fluorochromes, calcein and alizarin complexone, which are known to bind precipitated mineral, by confocal microscopy in undecalcified femur middiaphysis sections (Fig. 5*A*). Mineral apposition rate is the rate at which new bone is mineralized. It is calculated by dividing the mean measured distance between the inner perimeters of the two fluorochrome bands by the interval of time elapsed between the two dosings of flourochromes (65). Mineral apposition rate calculated from the images showed a significant increase in bones of mice treated with PEG-SMLA (Fig. 5*B*).

These results, together with the data obtained by the μCT, suggested that blocking of leptin signaling leads to enhanced bone formation and resorption in young mice. After several short-term experiments with 2- to 3-mo-old mice, we show for the first time that to obtain the effects of leptin inhibition on bone metabolism, it is very important to start the treatment at an early age when the bone is still in the growth stage, as opposed to *ob/ob* mice, where the leptin deficiency state is from birth, and thus the effects of leptin treatment on bones in these mice are more dramatic.

DISCUSSION

The effect of obesity on bone physiology has been widely studied and debated (11, 14, 24, 70, 71), with comparisons of phenotypes of various animal models and epidemiological data revealing a fertile research area. In this work, we used a unique model of transient intervention in leptin signaling, leading to modifications in metabolism and eating behavior. We employed a superactive leptin antagonist that has been shown to cause dramatic and rapid weight gain (27, 82) to study its metabolic and bone phenotypes compared with the genetic (*ob/ob* and *db/db*) and nutritional (diet-induced obesity) models.

A high-fat diet (HFD) followed by diet-induced obesity (DIO) is a widely used method for studying nutritional effects on the development of metabolic syndrome, which may eventually lead to T2DM. Here, we compared several metabolic and bone parameters and the expression of several genes in adi-

Table 3. *Cortical morphological characteristics*

	4 wk		12 wk	
	Control	PEG-SMLA	Control	PEG-SMLA
AIP, μm^2	1.04 ± 0.02	1.21 ± 0.03*	1.19 ± 0.04	1.4 ± 0.05*
CS.Ar, μm^2	0.57 ± 0.01	0.65 ± 0.01*	0.72 ± 0.03	0.84 ± 0.03*
Med.Ar, μm^2	0.47 ± 0.01	0.57 ± 0.02*	0.47 ± 0.02	0.57 ± 0.02*
Cor.Th, μm	0.2 ± 0.002	0.2 ± 0.002	0.22 ± 0.001	0.23 ± 0.003
MMIpolar, μm^4	0.15 ± 0.005	0.218 ± 0.01*	0.243 ± 0.02	0.343 ± 0.02*
BMD, g/cm^3	1.01 ± 0.03	0.97 ± 0.006*	1.06 ± 0.02	0.98 ± 0.008*

Data show means ± SE; $n = 11$. *$P < 0.05$ vs. control.AIP, area inside the periosteum; CS.Ar, cross-sectional area; Med.Ar, medullary area; Cor.Th, cortical thickness; MMIpolar, polar moment of inertia; BMD, bone mineral density.

Table 4. *Cortical 3-point bending test on tibiae from control and PEG-SMLA groups*

	4 wk		12 wk	
	Control	PEG-SMLA	Control	PEG-SMLA
F_{max}, N	19.19 ± 0.43	21.07 ± 0.5*	24.3 ± 1.62	27.56 ± 0.77
Stiffness, N/mm	0.105 ± 0.004	0.12 ± 0.005*	0.13 ± 0.01	0.16 ± 0.001
AUC, N/mm	8,039 ± 745.5	10,513.6 ± 758.7*	9,903.2 ± 1,096	11,097.2 ± 664
$F_{fracture}$, N	14.70 ± 0.7	15.27 ± 0.7	18.41 ± 2.5	20.2 ± 1.0
F_{yield}, N	14.65 ± 0.37	16.25 ± 0.41*	16.5 ± 0.7	21.6 ± 0.62*

Data show means ± SE; $n = 11$. *$P < 0.05$.

F_{max}, maximal load; AUC, area under the curve; $F_{fracture}$, load to fracture; F_{yield}, yield load.

pose, liver, muscle, and brain tissues in our model with those reported by others under various HFD regimes. We limited our comparison to C57BL/6J mice, a strain that is known to be susceptible to diabetes on HFDs and is the genetic background for the *ob/ob* model; the results are compiled in Supplemental Table S2. The absolute weight gain in both HFD and PEG-SMLA treatments was similar, but the latter was achieved in 2–3 wk, in contrast to the much longer period required with a HFD (8, 13, 14, 34, 37, 39, 40, 55, 58, 64, 69), and the outcome could be rapidly reversed (27). However, the feeding behavior was different. Under a HFD, energy intake parallels the controls for the first 4 wk and then gradually increases to about 15 to 20% above controls (54, 55, 58). In contrast, PEG-SMLA-treated mice eat regular chow but increase their food intake by 75–80% from the first days for 2 or 3 wk. Then it gradually decreases to control levels despite the continuous weight gain.

The changes in the various blood parameters, such as levels of triglycerides, cholesterol, and insulin, were similar between the HFD and PEG-SMLA treatments, although glucose levels were higher in HFD (8, 39, 40, 58). A comparison of two inflammatory cytokines showed a similar pattern. IL-6 increased 1.4- to fivefold in HFD after 5–24 wk (18, 53, 69), whereas with the PEG-SMLA treatment it increased 1.6-fold after 12 wk. TNFα increased two- to fourfold after 5–15 wk

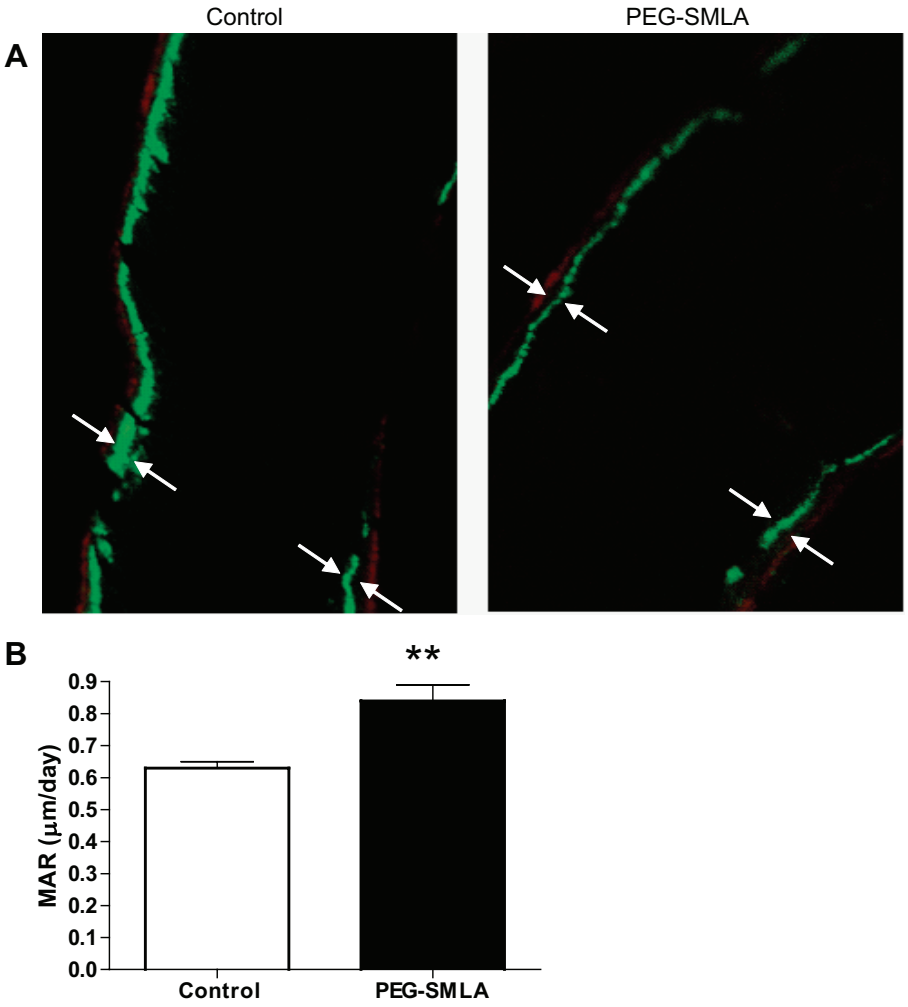

Fig. 5. Undecalcified femur middiaphysis sections from control and PEG-SMLA-treated mice. Mice were injected sc with calcein (15 mg/kg) on *day 20* and alizarin complexone (10 mg/kg) on *day 26*. *A*: undecalcified femur middiaphysis sections from control and PEG-SMLA after 4 wk; magnification, ×2.5. Arrows indicate suitable sites of double labels as used for mineral apposition rate (MAR) measurements. *B*: calculation of MAR. Treatment vs. control; **$P < 0.01$.

with the HFD (18, 21, 53, 59), whereas in the PEG-SMLA treatment it was unchanged after 4 wk and increased 4.8-fold after 12 wk. However, in a shorter PEG-SMLA treatment with murine urokinase-like plasminogen activator (αMUPA) and FVB/N (WT) mice, the blood level of those cytokines was not significantly changed (16). Serum alanine aminotransferase was increased 1.3- to 2.0-fold with a HFD after 18 wk and aspartate aminotransferase two- to 2.6-fold after 15 wk (43, 44). In contrast, PEG-SMLA treatment in C57BL/6J and αMUPA mice did not change the levels of these hepatic enzymes.

In the present work, we analyzed the expression of more than 77 genes in adipose tissue, muscle, liver, and brain. The expression of most of the tested genes from adipose tissue and muscle showed a high degree of similarity between HFD and PEG-SMLA treatments. Of particular interest was the common effect on the expression of *SIRT1* and *PPARγ*. The latter is upregulated in cells that have high insulin resistance (41). *SIRT1* is known to trigger fat mobilization by inhibiting *PPARγ* (67). Its decrease in both diets might explain the increased *PPARγ* expression in the WAT, which may induce and accelerate adipocyte differentiation and fat storage. It is also consistent with the finding that *PPARγ* binds to *cis*-elements on the insulin-dependent *GLUT4* promoter, keeping it in a repressed state and resulting in insulin resistance (45). The most unexpected finding, however, was the decrease in the gene expression of both *FASN* and its regulating protein sterol regulatory element-binding transcription factor 1 (*SREBF1*), whose expression is known to be regulated by insulin (31), in the PEG-SMLA treatment, in contrast to a respective 10- and threefold increase in HFD (52). Interestingly, in *ob/ob* mice, *SREBF1* and *FASN* gene expression in the adipose tissue decreases 1.5- to fourfold and 10-fold, respectively (92). These results hint at possible blockage of leptin action by PEG-SMLA or lack of leptin in *ob/ob* mice, rather than obesity, being responsible for this difference. This also contradicts the report of leptin decreasing the expression of *FASN* in epididymal adipose tissue in male Sprague-Dawley rats (3). Another unexplained difference was the decrease in adiponectin expression with a HFD in contrast to no change, or even an increase, in the PEG-SMLA treatment. In *ob/ob* mice, adiponectin is either undetectable or decreased (20).

In most cases, gene expression in the liver of PEG-SMLA- and HFD-treated mice showed a similar trend. However, in a few cases, an opposite readout was found; expression of the gene encoding *PEPCK*, which catalyzes the rate-controlling step in gluconeogenesis (9), was elevated in the liver of HFD mice (1), a feature characteristic of prediabetic or diabetic stages, but decreased in PEG-SMLA-treated mice, where leptin blocking may be responsible for this effect. Notably, PEG-SMLA treatment also led to a decrease in other gluconeogenesis-related genes in the liver such as *PGC-1α*, *PEPCK*, and *Fbp1* (see Supplemental Table S2). It is difficult to compare our results with those of *ob/ob* mice because of controversial reports regarding *PEPCK* gene expression in the latter, with some reporting a 1.5- to sixfold increase (42, 75) whereas others report a three- to 11-fold decrease (6, 30). Another gene of interest is the liver X receptor (*LXRα*), which is an important regulator of cholesterol, fatty acid, and glucose homeostasis (19). *LXRα*-knockout mice have been reported to develop enlarged fatty livers when fed a high-cholesterol diet (66), suggesting its role in the development of metabolic disorders such as hyperlipidemia and atherosclerosis. As shown in Table 6, a HFD leads to a 2.5-fold increase in *LXRα* expression in the liver in contrast to PEG-SMLA treatment, which led to downregulation of *LXRα* after 4 wk but little change after 12 wk. These results suggest that in the PEG-SMLA treatment there is no cholesterol overload in the liver. In contrast, in *ob/ob* mice, *LXRα* expression increased 1.3-fold (78). *LPL* gene expression in the liver of mice under a HFD increased 1.2- to twofold (29, 69), whereas with the PEG-SMLA treatment its expression was decreased after 4 wk. *RIFL* is a prolipogenic gene that is highly induced during adipocyte differentiation, indicating enhanced adipogenesis, which is consistent with the expression of other genes responsible for adipogenesis in our study. Expression of *RIFL* transcript in the liver of *ob/ob* compared with WT mice is significantly increased, ~4.5-fold (74). Its expression is induced during adipogenesis in rodent and human model systems and is correlated with lipid levels (74). In our study, *RIFL* expression did not change significantly. We have not been able to find any published data on its expression under a HFD. Another remarkable difference in genes expressed in the liver was the case in *CD14* and *TLR4*. *CD14* acts as a coreceptor (along with *TLR4* and *MD-2*) for the detection of bacterial lipopolysaccharide (48). A HFD has recently been reported to increase the expression of both *CD14* and *TLR4* (both located in liver Kuffer cells and related to increased sensitivity to inflammation), and it was suggested that increased leptin levels in HFD are responsible for this effect (38). *CD14* gene expression in the *ob/ob* mouse liver decreased twofold (79), similar to PEG-SMLA treatment, in which we reported a 1.6- to 2.4-fold decrease. *TLR4* gene expression in *ob/ob* mice was unchanged (79), similar to its expression in PEG-SMLA treatment, despite the obese phenotype, further supporting the suggested role of leptin as an inflammatory mediator. Notably, the decreased expression of hepatic *CD14* gene in *ob/ob* mice could be ameliorated by exogenous leptin (38). In conclusion, out of more than 75 genes tested, seven showed opposite effects of HFD and PEG-SMLA treatment.

Notable differences in the effects of HFD and PEG-SMLA treatment on bone parameters were also observed. Bone analyses in our and others' studies included the trabecular bone parameters, tested in the trabecular area of the tibiae and vertebrae, mostly in the LV3 and LV4, which are susceptible to osteoporotic fractures in humans. Whereas HFD was shown to decrease both trabecular thickness and number and, as a result, the volume of bone in the vertebrae (BV/TV) by 20–30% (12, 13, 34, 64), our results showed a rapid increase of 25–32% in BV/TV when treatment with PEG-SMLA was started at a young age. These results are in better agreement with the bone phenotypes described in the *ob/ob* models in reports from Ducy et al. (24), Karsenty (46), and Takeda et al. (87) but not from Bartell et al. (7) or Steppan et al. (85). Cortical bone analysis (tested in the tibia and the LV3) includes morphological parameters, calculation of mineral density, and mechanical tests. In some of these parameters, the results from the HFD models do not agree with our findings. For instance, we demonstrate an increase in medullary area, whereas in HFD the medullary area is not modified (12); we demonstrate an increase in cross-sectional area, whereas in HFD some report an increase in cross-sectional area (39, 58), and others report a decrease (34). With PEG-SMLA, cortical thickness did not change, whereas in HFD it increased or was unchanged (12,

39). With PEG-SMLA, long bone stiffness and maximal load increased, whereas they decreased in HFD models (39, 40). These results again imply that blocking leptin signaling differs from human obesity, which is largely diet induced. Obesity is strongly correlated with increased BMD measured by dual-energy X-ray absorptiometry and reduced osteoporotic fractures in postmenopausal women (72, 73). This association can be explained partially by the mechanical loading effects of increased BW (5); however, other factors have been postulated to play a role, such as increased production of proinflammatory cytokines, a hallmark of DIO induced by HFD, and adipose tissue-associated hormonal factors, including estrogen, leptin, and adiponectin (2, 73, 76, 77). The fact that leptin does not affect all bones similarly is an intriguing subject that may also explain some of the controversy in this field. However, in our model the effect of the antagonist was similar in the different bones. It increased BV/TV of trabecular bones and the thickness of the cortical bones in the vertebra as well as in tibia. This has contradicted some of the results published by Hamrick et al. (36), which show varied leptin signaling between different skeletal regions and moieties. They showed that *ob/ob* had lower femoral BMD but higher lumbar BMD compared with WT mice, whereas cortical thickness was reduced in both sites, suggesting that the effects of altered leptin signaling on bone differ significantly between axial and appendicular regions.

We can suggest an explanation for these differences. Hamrick et al. (36) used *ob/ob* mice, which do not express leptin at all times, from embryonic stages, whereas we used WT mice that until the age of 4 wk have a normal leptin signal during major periods of development. Because bone reactions depend on the initiation of the blocking treatments (1 vs. 2 mo), it is not unexpected that complete absence vs. temporary leptin signaling blocking results in different outcomes, supporting the complexity of leptin effect on bone.

In our previous studies, proinflammatory cytokines were suggested to decrease bone formation (15, 83). It seems that one of the major differences between DIO and leptin signaling-deficient obesity due to PEG-SMLA treatment is the inflammatory condition. Circulating inflammatory cytokines are higher in DIO compared with normal subjects (18, 53, 59, 69). With respect to leptin signaling, we showed that chronic inflammation is alleviated in leptin antagonist-treated mice (26, 27); this might explain the differences found in bone phenotype between the two models.

Leptin, the major cytokine secreted from the adipose tissue, is suggested to be the key regulator of both energy and bone metabolism. Increased levels of leptin and insulin in states of obesity may serve to either increase or decrease bone turnover, depending on the state of resistance to these hormones in the various cells of the bones. Although the present PEG-SMLA model does not resolve the debate regarding leptin's peripheral vs. central effect on bones since PEG-SMLA blocks leptin signaling in the periphery as well as through the hypothalamus (27), it blocks leptin signaling on a physiological background, which enables intervention at different time points and for different periods of time. This experimental tool allows us to distinguish between leptin's roles during the developmental or maturation phase of bones in contrast to knockout mice that differ substantially from the WT due to compensatory mechanisms evolved in these models. Indeed, our results demonstrate that, unlike the metabolic phenotype, bone phenotype depends substantially on age at treatment initiation. Leptin blocking had a dramatic effect on food consumption, BW, and metabolic parameters at various ages, representing childhood (1 mo), adolescence and early sexual maturation (3 mo), and adulthood (6 mo). However, the effect of PEG-SMLA on bone parameters was significantly positive only upon initiation of treatment immediately postweaning; it had little or no effect on the skeleton when treatment was initiated later. Skeleton is an example of tissue that continues its developmental processes in the postnatal period (especially the long bones) until sexual maturation, when the growth plate ceases growth, through chondrocyte terminal differentiation and apoptosis. Although there are differences between different species in timing and process of growth plate closure, the above-mentioned ages of 4 and 12 wk represent periods of "childhood" and young puberty in terms of bone elongation and development. Thus we assume that the effects we observe when injections begin earlier but not when experiments started later account for the differences in bone maturity. Processes that occur earlier are related to bone modeling and later to bone remodeling.

It is important to note that obesity is an endocrine condition/pathology and that its hallmark is insulin resistance and a low-grade inflammation. Obese subjects have moderate increases in circulating levels of inflammatory mediators, in addition to leptin, that originate from the white adipose tissue, some of which influence insulin sensitivity and glucose metabolism, creating insulin resistance, which is a cardinal feature in the development of the metabolic syndrome, but they also affect bone development and quality. The process of bone development is governed by a complex network of endocrine signals, including insulin, growth hormone (GH), IGF-I, glucocorticoid, estrogen, vitamin D, and leptin, acting both locally on bone cells and indirectly by modulating other signals in the network. Any disturbance in these tightly regulated processes results in skeletal growth anomalies (49, 50). Additionally, GH and IGF-I, which are known modulators of bone growth, have a dramatic effect on the balance of adipose tissue development and maintenance interacting with leptin activity to control bone, adipose, and muscle tissues in a complex system (28). GH not only is the regulator bone elongation but also affects bone remodeling and mineralization, and impairment of bone strength in GH deficiency may also be related to its metabolic effects (63, 86). Earlier, we demonstrated the regulation of bone development by GH, FGF (61, 91), and factors related to alteration in the body metabolic status such as adiponectin and interleukin-1β, which was produced and secreted from the adipose tissue (15, 83, 84).

Our previous (27, 82) and present studies and our unpublished data stem from female and male C57BL/6J mice, but the rapid and reversible weight gain induced by PEG-SMLA injections is not confined to this strain. In another study using 3- or 5-mo-old FVB/N (WT) mice and αMUPA lean mice derived from that strain, a rapid ≤40% weight gain was also observed (16). Similar results were also obtained with 2-mo-old 129/SvJ (WT) male mice and PRLR-knockout mice derived from that strain (Binart N, Solomon G, and Gertler A, unpublished observations). However, in contrast to the weight gain effect of PEG-SMLA that is common to all tested strains, the subsequent transition to metabolic syndrome as reflected by the increase in blood insulin and HOMA-IR differs. The highest increase, up to five- or sixfold, was observed in

C57BL/6J and αMUPA mice, whereas the increase in old FVB/N (WT) mice was only 2.6-fold, and in 129/SvJ (WT) and PRLR-knockout mice it was less than twofold (Binart N and Gertler A, unpublished observations).

In summary, PEG-SMLA treatment leads to a new model of obesity, metabolic syndrome, and borderline T2DM. It is also less inflammatory than the HFD model, which is most likely due to the blocking of proinflammatory leptin action. Thus our model differs from the existing genetic nonreversible or slow DIO HFD models, as it is fast, reversible, and physiologically different. It is also suitable for the study of adipogenesis and bone development maturation.

ACKNOWLEDGMENTS

We are thankful to Sveta Pen from the Hebrew University, Israel, for assistance during the work on this article.

GRANTS

This work was partially supported by Nutricia Grant No. 2012-23 and by Israel Science Foundation Grant No. 1050/13.

DISCLOSURES

No conflicts of interest, financial or otherwise, are declared by the authors.

AUTHOR CONTRIBUTIONS

G.S., A.G., and E.M.-O. contributed to the conception and design of the research; G.S. performed the experiments; G.S., A.A., R.S., A.G., and E.M.-O. analyzed the data; G.S., A.A., R.S., A.G., and E.M.-O. interpreted the results of the experiments; G.S. and E.M.-O. prepared the figures; G.S., A.G., and E.M.-O. drafted the manuscript; G.S., R.S., A.G., and E.M.-O. edited and revised the manuscript; A.G. and E.M.-O. approved the final version of the manuscript.

REFERENCES

1. **Ables GP, Perrone CE, Orentreich D, Orentreich N.** Methionine-restricted C57BL/6J mice are resistant to diet-induced obesity and insulin resistance but have low bone density. *PLoS One* 7: e51357, 2012.
2. **Albala C, Yanez M, Devoto E, Sostin C, Zeballos L, Santos JL.** Obesity as a protective factor for postmenopausal osteoporosis. *Int J Obes Relat Metab Disord* 20: 1027–1032, 1996.
3. **Ambati S, Li Q, Rayalam S, Hartzell DL, Della-Fera MA, Hamrick MW, Baile CA.** Central leptin versus ghrelin: effects on bone marrow adiposity and gene expression. *Endocrine* 37: 115–123, 2010.
4. **Amling M, Takeda S, Karsenty G.** A neuro (endo)crine regulation of bone remodeling. *Bioessays* 22: 970–975, 2000.
5. **Ağbaht K, Gürlek A, Karakaya J, Bayraktar M.** Circulating adiponectin represents a biomarker of the association between adiposity and bone mineral density. *Endocrine* 35: 371–379, 2009.
6. **Barros CC, Haro A, Russo FJ, Schadock I, Almeida SS, Reis FC, Moraes MR, Haidar A, Hirata AE, Mori M, Bacurau RF, Würtele M, Bader M, Pesquero JB, Araujo RC.** Bradykinin inhibits hepatic gluconeogenesis in obese mice. *Lab Invest* 92: 1419–1427, 2012.
7. **Bartell SM, Rayalam S, Ambati S, Gaddam DR, Hartzell DL, Hamrick M, She JX, Della-Fera MA, Baile CA.** Central (ICV) leptin injection increases bone formation, bone mineral density, muscle mass, serum IGF-1, and the expression of osteogenic genes in leptin-deficient ob/ob mice. *J Bone Miner Res* 26: 1710–1720, 2011.
8. **Bartelt A, Beil FT, Schinke T, Roeser K, Ruether W, Heeren J, Niemeier A.** Apolipoprotein E-dependent inverse regulation of vertebral bone and adipose tissue mass in C57Bl/6 mice: modulation by diet-induced obesity. *Bone* 47: 736–745, 2010.
9. **Barthel A, Schmoll D.** Novel concepts in insulin regulation of hepatic gluconeogenesis. *Am J Physiol Endocrinol Metab* 285: E685–E692, 2003.
10. **Cakir I, Perello M, Lansari O, Messier NJ, Vaslet CA, Nillni EA.** Hypothalamic Sirt1 regulates food intake in a rodent model system. *PLoS One* 4: e8322, 2009.
11. **Cao JJ.** Effects of obesity on bone metabolism. *J Orthop Surg Res* 6: 30, 2011.
12. **Cao JJ, Gregoire BR, Gao H.** High-fat diet decreases cancellous bone mass but has no effect on cortical bone mass in the tibia in mice. *Bone* 44: 1097–1104, 2009.
13. **Cao JJ, Sun L, Gao H.** Diet-induced obesity alters bone remodeling leading to decreased femoral trabecular bone mass in mice. *Ann NY Acad Sci* 1192: 292–297, 2010.
14. **Carson EA, Kenney-Hunt JP, Pavlicev M, Bouckaert KA, Chinn AJ, Silva MJ, Cheverud JM.** Weak genetic relationship between trabecular bone morphology and obesity in mice. *Bone* 51: 46–53, 2012.
15. **Challa TD, Rais Y, Ornan EM.** Effect of adiponectin on ATDC5 proliferation, differentiation and signaling pathways. *Mol Cell Endocrinol* 323: 282–291, 2010.
16. **Chapnik N, Solomon G, Genzer Y, Miskin R, Gertler A, Froy O.** A superactive leptin antagonist alters metabolism and locomotion in high-leptin mice. *J Endocrinol* 217: 283–290, 2013.
18. **Choi Y, Kim Y, Park S, Lee KW, Park T.** Indole-3-carbinol prevents diet-induced obesity through modulation of multiple genes related to adipogenesis, thermogenesis or inflammation in the visceral adipose tissue of mice. *J Nutr Biochem* 23: 1732–1739, 2012.
19. **Chuu CP, Kokontis JM, Hiipakka RA, Liao S.** Modulation of liver X receptor signaling as novel therapy for prostate cancer. *J Biomed Sci* 14: 543–553, 2007.
20. **Delporte ML, El Mkadem SA, Quisquater M, Brichard SM.** Leptin treatment markedly increased plasma adiponectin but barely decreased plasma resistin of *ob/ob* mice. *Am J Physiol Endocrinol Metab* 287: E446–E453, 2004.
21. **Diaz-Delfin J, Hondares E, Iglesias R, Giralt M, Caelles C, Villarroya F.** TNF-alpha represses beta-Klotho expression and impairs FGF21 action in adipose cells: involvement of JNK1 in the FGF21 pathway. *Endocrinology* 153: 4238–4245, 2012.
22. **Dietrich MO, Antunes C, Geliang G, Liu ZW, Borok E, Nie Y, Xu AW, Souza DO, Gao Q, Diano S, Gao XB, Horvath TL.** Agrp neurons mediate Sirt1's action on the melanocortin system and energy balance: roles for Sirt1 in neuronal firing and synaptic plasticity. *J Neurosci* 30: 11815–11825, 2010.
23. **Douen AG, Ramlal T, Rastogi S, Bilan PJ, Cartee GD, Vranic M, Holloszy JO, Klip A.** Exercise induces recruitment of the "insulin-responsive glucose transporter". Evidence for distinct intracellular insulin- and exercise-recruitable transporter pools in skeletal muscle. *J Biol Chem* 265: 13427–13430, 1990.
24. **Ducy P, Amling M, Takeda S, Priemel M, Schilling AF, Beil FT, Shen J, Vinson C, Rueger JM, Karsenty G.** Leptin inhibits bone formation through a hypothalamic relay: a central control of bone mass. *Cell* 100: 197–207, 2000.
25. **Elefteriou F, Takeda S, Ebihara K, Magre J, Patano N, Kim CA, Ogawa Y, Liu X, Ware SM, Craigen WJ, Robert JJ, Vinson C, Nakao K, Capeau J, Karsenty G.** Serum leptin level is a regulator of bone mass. *Proc Natl Acad Sci USA* 101: 3258–3263, 2004.
26. **Elinav E, Ali M, Bruck R, Brazowski E, Phillips A, Shapira Y, Katz M, Solomon G, Halpern Z, Gertler A.** Competitive inhibition of leptin signaling results in amelioration of liver fibrosis through modulation of stellate cell function. *Hepatology* 49: 278–286, 2009.
27. **Elinav E, Niv-Spector L, Katz M, Price TO, Ali M, Yacobovitz M, Solomon G, Reicher S, Lynch JL, Halpern Z, Banks WA, Gertler A.** Pegylated leptin antagonist is a potent orexigenic agent: preparation and mechanism of activity. *Endocrinology* 150: 3083–3091, 2009.
28. **Evans BA, Bull MJ, Kench RC, Fox RE, Morgan LD, Stevenson AE, Gevers EF, Perry MJ, Wells T.** The influence of leptin on trabecular architecture and marrow adiposity in GH-deficient rats. *J Endocrinol* 208: 69–79, 2011.
29. **Fan S, Zhang Y, Hu N, Sun Q, Ding X, Li G, Zheng B, Gu M, Huang F, Sun YQ, Zhou Z, Lu X, Huang C, Ji G.** Extract of Kuding tea prevents high-fat diet-induced metabolic disorders in C57BL/6 mice via liver X receptor (LXR) beta antagonism. *PLoS One* 7: e51007, 2012.
30. **Ferber S, Meyerovitch J, Kriauciunas KM, Kahn CR.** Vanadate normalizes hyperglycemia and phosphoenolpyruvate carboxykinase mRNA levels in ob/ob mice. *Metabolism* 43: 1346–1354, 1994.
31. **Ferré P, Foufelle F.** Hepatic steatosis: a role for de novo lipogenesis and the transcription factor SREBP-1c. *Diabetes Obes Metab* 12, *Suppl* 2: 83–92, 2010.
32. **Friedman JM, Halaas JL.** Leptin and the regulation of body weight in mammals. *Nature* 395: 763–770, 1998.
33. **Fruhbeck G.** Intracellular signalling pathways activated by leptin. *Biochem J* 393: 7–20, 2006.

34. **Fujita Y, Watanabe K, Maki K.** Serum leptin levels negatively correlate with trabecular bone mineral density in high-fat diet-induced obesity mice. *J Musculoskelet Neuronal Interact* 12: 84–94, 2012.
35. **Hamrick MW, Della-Fera MA, Choi YH, Pennington C, Hartzell D, Baile CA.** Leptin treatment induces loss of bone marrow adipocytes and increases bone formation in leptin-deficient ob/ob mice. *J Bone Miner Res* 20: 994–1001, 2005.
36. **Hamrick MW, Pennington C, Newton D, Xie D, Isales C.** Leptin deficiency produces contrasting phenotypes in bones of the limb and spine. *Bone* 34: 376–383, 2004.
37. **Heep H, Wedemeyer C, Wegner A, Hofmeister S, von Knoch M.** Differences in trabecular bone of leptin-deficient ob/ob mice in response to biomechanical loading. *Int J Biol Sci* 4: 169–175, 2008.
38. **Imajo K, Fujita K, Yoneda M, Nozaki Y, Ogawa Y, Shinohara Y, Kato S, Mawatari H, Shibata W, Kitani H, Ikejima K, Kirikoshi H, Nakajima N, Saito S, Maeyama S, Watanabe S, Wada K, Nakajima A.** Hyperresponsivity to low-dose endotoxin during progression to nonalcoholic steatohepatitis is regulated by leptin-mediated signaling. *Cell Metab* 16: 44–54, 2012.
39. **Ionova-Martin SS, Do SH, Barth HD, Szadkowska M, Porter AE, Ager JW 3rd, Ager JW Jr, Alliston T, Vaisse C, Ritchie RO.** Reduced size-independent mechanical properties of cortical bone in high-fat diet-induced obesity. *Bone* 46: 217–225, 2010.
40. **Ionova-Martin SS, Wade JM, Tang S, Shahnazari M, Ager JW 3rd, Lane NE, Yao W, Alliston T, Vaisse C, Ritchie RO.** Changes in cortical bone response to high-fat diet from adolescence to adulthood in mice. *Osteoporos Int* 22: 2283–2293, 2011.
41. **Jones JR, Barrick C, Kim KA, Lindner J, Blondeau B, Fujimoto Y, Shiota M, Kesterson RA, Kahn BB, Magnuson MA.** Deletion of PPARgamma in adipose tissues of mice protects against high fat diet-induced obesity and insulin resistance. *Proc Natl Acad Sci USA* 102: 6207–6212, 2005.
42. **Kaidanovich-Beilin O, Eldar-Finkelman H.** Long-term treatment with novel glycogen synthase kinase-3 inhibitor improves glucose homeostasis in ob/ob mice: molecular characterization in liver and muscle. *J Pharmacol Exp Ther* 316: 17–24, 2006.
43. **Kang JS, Lee WK, Yoon WK, Kim N, Park SK, Park HK, Ly SY, Han SB, Yun J, Lee CW, Lee K, Lee KH, Park SK, Kim HM.** A combination of grape extract, green tea extract and L-carnitine improves high-fat diet-induced obesity, hyperlipidemia and non-alcoholic fatty liver disease in mice. *Phytother Res* 25: 1789–1795, 2011.
44. **Kang SI, Shin HS, Kim HM, Hong YS, Yoon SA, Kang SW, Kim JH, Ko HC, Kim SJ.** Anti-obesity properties of a Sasa quelpaertensis extract in high-fat diet-induced obese mice. *Biosci Biotechnol Biochem* 76: 755–761, 2012.
45. **Karnieli E, Armoni M.** Transcriptional regulation of the insulin-responsive glucose transporter GLUT4 gene: from physiology to pathology. *Am J Physiol Endocrinol Metab* 295: E38–E45, 2008.
46. **Karsenty G.** Leptin controls bone formation through a hypothalamic relay. *Recent Prog Horm Res* 56: 401–415, 2001.
47. **Livak KJ, Schmittgen TD.** Analysis of relative gene expression data using real-time Quantitative PCR and the 2(−Delta Delta C(T)) Method. *Methods* 25: 402–408, 2001.
48. **Kitchens RL.** Role of CD14 in cellular recognition of bacterial lipopolysaccharides. *Chem Immunol* 74: 61–82, 2000.
49. **Kobayashi T, Kronenberg H.** Minireview: transcriptional regulation in development of bone. *Endocrinology* 146: 1012–1017, 2005.
50. **Kronenberg HM.** Developmental regulation of the growth plate. *Nature* 423: 332–336, 2003.
51. **Kume K, Satomura K, Nishisho S, Kitaoka E, Yamanouchi K, Tobiume S, Nagayama M.** Potential role of leptin in endochondral ossification. *J Histochem Cytochem* 50: 159–169, 2002.
52. **Lee MS, Kim CT, Kim Y.** Green tea (−)-epigallocatechin-3-gallate reduces body weight with regulation of multiple genes expression in adipose tissue of diet-induced obese mice. *Ann Nutr Metab* 54: 151–157, 2009.
53. **Lee YS, Cha BY, Choi SS, Choi BK, Yonezawa T, Teruya T, Nagai K, Woo JT.** Nobiletin improves obesity and insulin resistance in high-fat diet-induced obese mice. *J Nutr Biochem* 24: 156–162, 2013.
54. **Li H, Xu M, Lee J, He C, Xie Z.** Leucine supplementation increases SIRT1 expression and prevents mitochondrial dysfunction and metabolic disorders in high-fat diet-induced obese mice. *Am J Physiol Endocrinol Metab* 303: E1234–E1244, 2012.
55. **Lin S, Thomas TC, Storlien LH, Huang XF.** Development of high fat diet-induced obesity and leptin resistance in C57Bl/6J mice. *Int J Obes Relat Metab Disord* 24: 639–646, 2000.
57. **Luquet S, Perez FA, Hnasko TS, Palmiter RD.** NPY/AgRP neurons are essential for feeding in adult mice but can be ablated in neonates. *Science* 310: 683–685, 2005.
58. **Ma H, Torvinen S, Silvennoinen M, Rinnankoski-Tuikka R, Kainulainen H, Morko J, Peng Z, Kujala UM, Rahkila P, Suominen H.** Effects of diet-induced obesity and voluntary wheel running on bone properties in young male C57BL/6J mice. *Calcif Tissue Int* 86: 411–419, 2010.
59. **Maeda H, Hosokawa M, Sashima T, Murakami-Funayama K, Miyashita K.** Anti-obesity and anti-diabetic effects of fucoxanthin on diet-induced obesity conditions in a murine model. *Mol Med Rep* 2: 897–902, 2009.
60. **Maor G, Rochwerger M, Segev Y, Phillip M.** Leptin acts as a growth factor on the chondrocytes of skeletal growth centers. *J Bone Miner Res* 17: 1034–1043, 2002.
61. **Monsonego-Ornan E, Adar R, Feferman T, Segev O, Yayon A.** The transmembrane mutation G380R in fibroblast growth factor receptor 3 uncouples ligand-mediated receptor activation from down-regulation. *Mol Cell Biol* 20: 516–522, 2000.
62. **Myers MG, Cowley MA, Munzberg H.** Mechanisms of leptin action and leptin resistance. *Annu Rev Physiol* 70: 537–556, 2008.
63. **Ohlsson C, Vidal O.** Effects of growth hormone and insulin-like growth factors on human osteoblasts. *Eur J Clin Invest* 28: 184–186, 1998.
64. **Patsch JM, Kiefer FW, Varga P, Pail P, Rauner M, Stupphann D, Resch H, Moser D, Zysset PK, Stulnig TM, Pietschmann P.** Increased bone resorption and impaired bone microarchitecture in short-term and extended high-fat diet-induced obesity. *Metabolism* 60: 243–249, 2011.
65. **Pautke C, Vogt S, Tischer T, Wexel G, Deppe H, Milz S, Schieker M, Kolk A.** Polychrome labeling of bone with seven different fluorochromes: enhancing fluorochrome discrimination by spectral image analysis. *Bone* 37: 441–445, 2005.
66. **Peet DJ, Turley SD, Ma W, Janowski BA, Lobaccaro JM, Hammer RE, Mangelsdorf DJ.** Cholesterol and bile acid metabolism are impaired in mice lacking the nuclear oxysterol receptor LXR alpha. *Cell* 93: 693–704, 1998.
67. **Picard F, Kurtev M, Chung N, Topark-Ngarm A, Senawong T, Machado De Oliveira R, Leid M, McBurney MW, Guarente L.** Sirt1 promotes fat mobilization in white adipocytes by repressing PPAR-gamma. *Nature* 429: 771–776, 2004.
68. **Pogoda P, Egermann M, Schnell JC, Priemel M, Schilling AF, Alini M, Schinke T, Rueger JM, Schneider E, Clarke I, Amling M.** Leptin inhibits bone formation not only in rodents, but also in sheep. *J Bone Miner Res* 21: 1591–1599, 2006.
69. **Premaratna SD, Manickam E, Begg DP, Rayment DJ, Hafandi A, Jois M, Cameron-Smith D, Weisinger RS.** Angiotensin-converting enzyme inhibition reverses diet-induced obesity, insulin resistance and inflammation in C57BL/6J mice. *Int J Obes (Lond)* 36: 233–243, 2012.
70. **Reid IR.** Fat and bone. *Arch Biochem Biophys* 503: 20–27, 2010.
71. **Reid IR.** Relationships among body mass, its components, and bone. *Bone* 31: 547–555, 2002.
72. **Reid IR, Evans MC, Ames RW.** Volumetric bone density of the lumbar spine is related to fat mass but not lean mass in normal postmenopausal women. *Osteoporos Int* 4: 362–367, 1994.
73. **Reid IR, Evans MC, Cooper GJ, Ames RW, Stapleton J.** Circulating insulin levels are related to bone density in normal postmenopausal women. *Am J Physiol Endocrinol Metab* 265: E655–E659, 1993.
74. **Ren G, Kim JY, Smas CM.** Identification of RIFL, a novel adipocyte-enriched insulin target gene with a role in lipid metabolism. *Am J Physiol Endocrinol Metab* 303: E334–E351, 2012.
75. **Reul BA, Becker DJ, Ongemba LN, Bailey CJ, Henquin JC, Brichard SM.** Improvement of glucose homeostasis and hepatic insulin resistance in ob/ob mice given oral molybdate. *J Endocrinol* 155: 55–64, 1997.
76. **Revilla M, Villa LF, Sanchez-Atrio A, Hernandez ER, Rico H.** Influence of body mass index on the age-related slope of total and regional bone mineral content. *Calcif Tissue Int* 61: 134–138, 1997.
77. **Ribot C, Tremollieres F, Pouilles JM.** The effect of obesity on postmenopausal bone loss and the risk of osteoporosis. *Adv Nutr Res* 9: 257–271, 1994.
78. **Roche HM, Noone E, Sewter C, Mc Bennett S, Savage D, Gibney MJ, O'Rahilly S, Vidal-Puig AJ.** Isomer-dependent metabolic effects of conjugated linoleic acid: insights from molecular markers sterol regulatory

element-binding protein-1c and LXRalpha. *Diabetes* 51: 2037–2044, 2002.

79. **Romics L Jr, Mandrekar P, Kodys K, Velayudham A, Drechsler Y, Dolganiuc A, Szabo G.** Increased lipopolysaccharide sensitivity in alcoholic fatty livers is independent of leptin deficiency and toll-like receptor 4 (TLR4) or TLR2 mRNA expression. *Alcohol Clin Exp Res* 29: 1018–1026, 2005.
80. **Salomon G, Niv-Spector L, Gussakovsky EE, Gertler A.** Large-scale preparation of biologically active mouse and rat leptins and their L39A/D40A/F41A muteins which act as potent antagonists. *Protein Expr Purif* 47: 128–136, 2006.
81. **Shen L, Tso P, Woods SC, Clegg DJ, Barber KL, Carey K, Liu M.** Brain apolipoprotein E: an important regulator of food intake in rats. *Diabetes* 57: 2092–2098, 2008.
82. **Shpilman M, Niv-Spector L, Katz M, Varol C, Solomon G, Ayalon-Soffer M, Boder E, Halpern Z, Elinav E, Gertler A.** Development and characterization of high affinity leptins and leptin antagonists. *J Biol Chem* 286: 4429–4442, 2011.
83. **Simsa-Maziel S, Monsonego-Ornan E.** Interleukin-1β promotes proliferation and inhibits differentiation of chondrocytes through a mechanism involving down-regulation of FGFR-3 and p21. *Endocrinology* 153: 2296–2310, 2012.
84. **Simsa-Maziel S, Zaretsky J, Reich A, Koren Y, Shahar R, Monsonego-Ornan E.** IL-1RI participates in normal growth plate development and bone modeling. *Am J Physiol Endocrinol Metab* 305: E15–E21, 2013.
85. **Steppan CM, Crawford DT, Chidsey-Frink KL, Ke H, Swick AG.** Leptin is a potent stimulator of bone growth in ob/ob mice. *Regul Pept* 92: 73–78, 2000.
86. **Stevenson AE, Evans BA, Gevers EF, Elford C, McLeod RW, Perry MJ, El-Kasti MM, Coschigano KT, Kopchick JJ, Evans SL, Wells T.** Does adiposity status influence femoral cortical strength in rodent models of growth hormone deficiency? *Am J Physiol Endocrinol Metab* 296: E147–E156, 2009.
87. **Takeda S, Elefteriou F, Levasseur R, Liu X, Zhao L, Parker KL, Armstrong D, Ducy P, Karsenty G.** Leptin regulates bone formation via the sympathetic nervous system. *Cell* 111: 305–317, 2002.
88. **Thomas T.** The complex effects of leptin on bone metabolism through multiple pathways. *Curr Opin Pharmacol* 4: 295–300, 2004.
89. **Turner CH, Burr DB.** Basic biomechanical measurements of bone: a tutorial. *Bone* 14: 595–608, 1993.
90. **Vessal M, Mishra S, Moulik S, Murphy LJ.** Prohibitin attenuates insulin-stimulated glucose and fatty acid oxidation in adipose tissue by inhibition of pyruvate carboxylase. *FEBS J* 273: 568–576, 2006.
91. **Weizmann S, Tong A, Reich A, Genina O, Yayon A, Monsonego-Ornan E.** FGF upregulates osteopontin in epiphyseal growth plate chondrocytes: implications for endochondral ossification. *Matrix Biol* 24: 520–529, 2005.
92. **Yahagi N, Shimano H, Hasty AH, Matsuzaka T, Ide T, Yoshikawa T, Amemiya-Kudo M, Tomita S, Okazaki H, Tamura Y, Iizuka Y, Ohashi K, Osuga J, Harada K, Gotoda T, Nagai R, Ishibashi S, Yamada N.** Absence of sterol regulatory element-binding protein-1 (SREBP-1) ameliorates fatty livers but not obesity or insulin resistance in Lep(ob)/Lep(ob) mice. *J Biol Chem* 277: 19353–19357, 2002.
93. **Zhang W, Ambati S, Della-Fera MA, Choi YH, Baile CA, Andacht TM.** Leptin modulated changes in adipose tissue protein expression in ob/ob mice. *Obesity (Silver Spring)* 19: 255–261, 2011.